Available online at www.sciencedirect.com
ScienceDirect
Trans. Nonferrous Met. Soc. China 21(2011) 322−329
Transactions of Nonferrous Metals Society of China
www.tnmsc.cn

Effect of annealing treatment on cyclic-oxidation of electrodeposited Ni-Al nanocomposite

ZHOU Yue-bo, ZHANG Hai-jun

College of Materials Science and Engineering, Heilongjiang Institute of Science and Technology, Harbin 150027, China

Received 21 January 2010; accepted 15 June 2010

Abstract: An electrodeposited Ni-Al nanocomposite having a nanocrystalline Ni matrix dispersing Al nanoparticles was annealed in vacuum at 500 °C for different time (3, 5 and 8 h, respectively). The results show that the annealing treatment leads to the reaction of Ni and Al to form intermetallics and the coarsened Ni grains that are doped with a certain amount of Al atoms diffused from the nanoparticles. Cyclic oxidation in air at 1 000 °C indicates that the scale spallation resistance of the annealed Ni-Al nanocomposite increases with the increase of annealing time, due to prevention of the composite intergranular cracking during the cycling, reduction of numerous surface NiO nodules formed on the scale spalled area and prevention of internal oxidation.
Key words: electrodeposition; nanocomposite; cyclic oxidation

1 Introduction

As is known, electrodeposition has the merits of simple processing and easy fabrication, low cost, high productivity, and good compositional control. Electrodeposited composite films consisting of a metal matrix with dispersed second-phase particles are frequently used as protective coatings for diverse purposes, such as wear resistance and antifriction due to their increased microhardness and improved wear resistance[1]. During the electrodeposition, these insoluble hard oxides or carbide particles, such as ZrO_2[2], Al_2O_3[3], La_2O_3[4] and SiC[5−7], are suspended in a conventional plating electrolyte and are captured in the growing metal film. Earlier works revealed that co-deposited SiC[7] or La_2O_3[4] particles improved the oxidation resistance of pure Ni. However, NiO scale intrinsically is not the thermally grown oxide (TGO) for providing an excellent oxidation resistance at high temperatures. For a desired TGO, it should be compact, slow-growing and thermodynamically stable. Two of these typical TGOs are chromium and alumina. In 1980s, FOSTER et al[8] firstly suggested that the coatings for oxidation resistance could be fabricated by co-electrodeposition of metal such as Ni with micrometer-sized metallic particles, such as CrAl or Al. However, the oxidation performance of such coatings has not been reported in detail due to a high density of defects (pinholes or pores) causing the quick penetration of oxygen into the coatings and preventing the protective scale from formation. In order to get coatings with oxidation resistance by codeposition, diffusion heat treatment[9−14] is a common processing before oxidation. Recently, a Ni-Al nanocomposite coating has been developed by codeposition of Ni with Al nanoparticles instead of the microscale countparts commonly used[15−17]. However, the electrodeposited Ni-Al nanocomposites exhibited bad cyclic oxidation resistance due to the formation of numerous NiO nodules on surface and internal oxidation of aluminum as a result of the composite intergranular cracking during the cycling; and the addition of CeO_2 nanoparticles significantly improved the cyclic oxidation resistance due to the intergranular cracking prevented[18]. Nevertheless, these reports[15−18] focused on the oxidation behavior of the nanocomposites in their as-deposited forms, a non-equilibrium state, at high temperatures. Lately, YANG et al[19−20] investigated the effect of the temperature on coarsening of Ni nanocrystals as well as the formation of intermetallics by the reaction of Al with Ni after annealing treatment on the isothermal-oxidation performance of an alumina-forming Ni-Al nanocomposite because similar structural

Foundation item: Project (11531319) supported by Scientific Research Fund of Heilongjiang Provincial Education Department, China; Project (06-13) supported by the Scientific Research Startup Foundation of Heilongjiang Institute of Science and Technology, China
Corresponding author: ZHOU Yue-bo; Tel: +86-451-88036159: E-mail: zhouyuebo760309@163.com; ybzhou@imr.ac.cn
DOI: 10.1016/S1003-6326(11)60716-4

evolution of the nanocomposites would occur during high temperature exposure. The results demonstrated that the annealing decreased the oxidation rate of the nanocomposite due to the accelerated development of the alumina layer on the annealed nanocomposite[19]. And the structure, not the Al content, has a great impact on the selective oxidation of Al to form a continuous alumina layer[20]. So far, the works in relation to the cyclic oxidation performance of the annealing alumina-forming Ni-Al nanocomposite has not been investigated. In this work, an electorodeposited Ni-Al nanocomposite (ENC Ni-Al) was heat-treated in vacuum at 500 ℃ for 3, 5 and 8 h, respectively; and the microstructures and cyclic oxidation behaviors of the ENC Ni-Al with and without annealing were investigated; the effect of annealing pretreatment time on the microstructure and the spallation resistance of the ENCs during cycling was focused.

2 Experimental

Specimens with the dimensions of 15 mm×10 mm×2 mm were cut from a pure electrolytic nickel plate (>99.9%). After being abraded with 800 grit SiC paper and ultrasonically cleaned in acetone, the specimens were electrodeposited (on all the sides) with ~40 μm-thick ENCs Ni-Al from a nickel sulfate bath containing 150 g/L $NiSO_4·7H_2O$, 15 g/L NH_4Cl, 15 g/L H_3BO_3, 0.1 g/L $C_{12}H_{25}NaSO_4$, and an appropriate content of Al nanoparticles. TEM results showed that the Al nanoparticles produced using a wire electrical explosion method were spherical and had a mean size of 100 nm based on the measurement from one hundred particles that were randomly selected[17]. The detail for producing the ENC has been reported elsewhere[15−17]. To guarantee a uniform distribution of the electrodeposited particles over the Ni matrix, the added particles were well dispersed in the bath during electrodeposition using a reciprocating perforated plastic plate. An alumina-forming ENC containing 14.0% Al (mass fraction) was screened out for the annealing treatment in this work according to ZHOU et al[15] and YANG et al[19]. It was conducted in a sealed quartz tube with a pressure of 133×10^{-4} Pa at 500 °C for 3, 5 and 8 h in order to form different Ni-Al composite coatings. To exclude the possible oxidation during annealing, the surface zone with a thickness of ~5 μm was removed from the annealed ENC (A-ENC) by grinding with 1 000 grit SiC paper. Cyclic oxidation at 1 000 °C in air was performed by automatically lifting samples from the hot zone of a vertical furnace after exposure for 45 min followed by a 15 min-cooling to room temperature. During oxidation, the samples were separately hung from the girder of small quartz baskets. After certain cycles, the samples were weighed using a balance with 0.01 mg sensitivity. The microstructures of the ENC and A-ENC before and after oxidation were comparatively investigated using X-ray diffraction (XRD), scanning and transmission electron microscopy (SEM, TEM), energy dispersive X-ray analysis (EDAX).

3 Results and discussion

3.1 Microstructure of coating

Fig.1 shows the XRD patterns of the ENC Ni-14Al before and after annealing at 500 °C for different time. It is evident that the annealing treatment causes the reaction of the codeposited Al nanoparticles with the Ni matrix to form new intermetallics phase such as δ-Ni_2Al_3 and γ'-Ni_3Al, and the position of the Ni peak corresponding one of ENC Ni-Al shifted to lower angles due to the larger Al atoms incorporating into the Ni lattice according to the Bragg equation. From Fig.1, it is also found that, the δ-Ni_2Al_3 peaks decrease and the γ'-Ni_3Al peaks increase with increasing annealing time. This suggests that the reaction of Al with Ni to form new intermetallics phase during annealing began from Al-rich intermetallics such as δ-Ni_2Al_3 to Ni-rich intermetallics (γ'-Ni_3Al), as reported elsewhere[21−23].

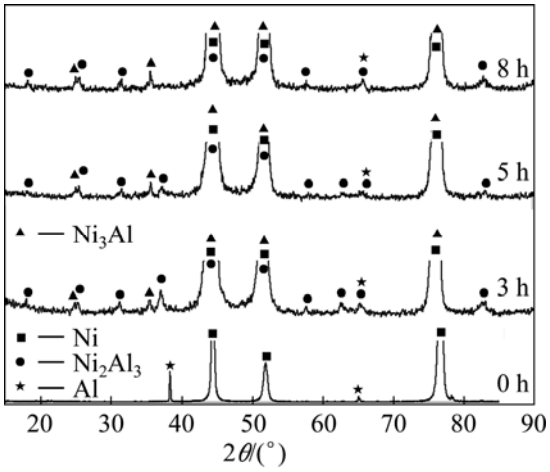

Fig.1 XRD pattern of ENC Ni-14Al before and after annealing at 500 °C for different time

Fig.2(a) shows the feature of the ENC Ni-14Al after polishing. The EDAX indicated that Al is richer in dark area than in light area. The Al nanoparticles are, in general, homogeneously dispersed in the coating, although some of them appear to be agglomerated into clusters. The fine structure of as-deposited Ni-Al nanocomposite can be seen from the TEM bright-field image in Fig.2(a′), where some nanoparticles of Al are indicated by solid circles. Generally, these nanoparticles are randomly dispersed in the nanocrystalline Ni matrix with the grain size of Ni ranging from15 to 60 nm. Twins

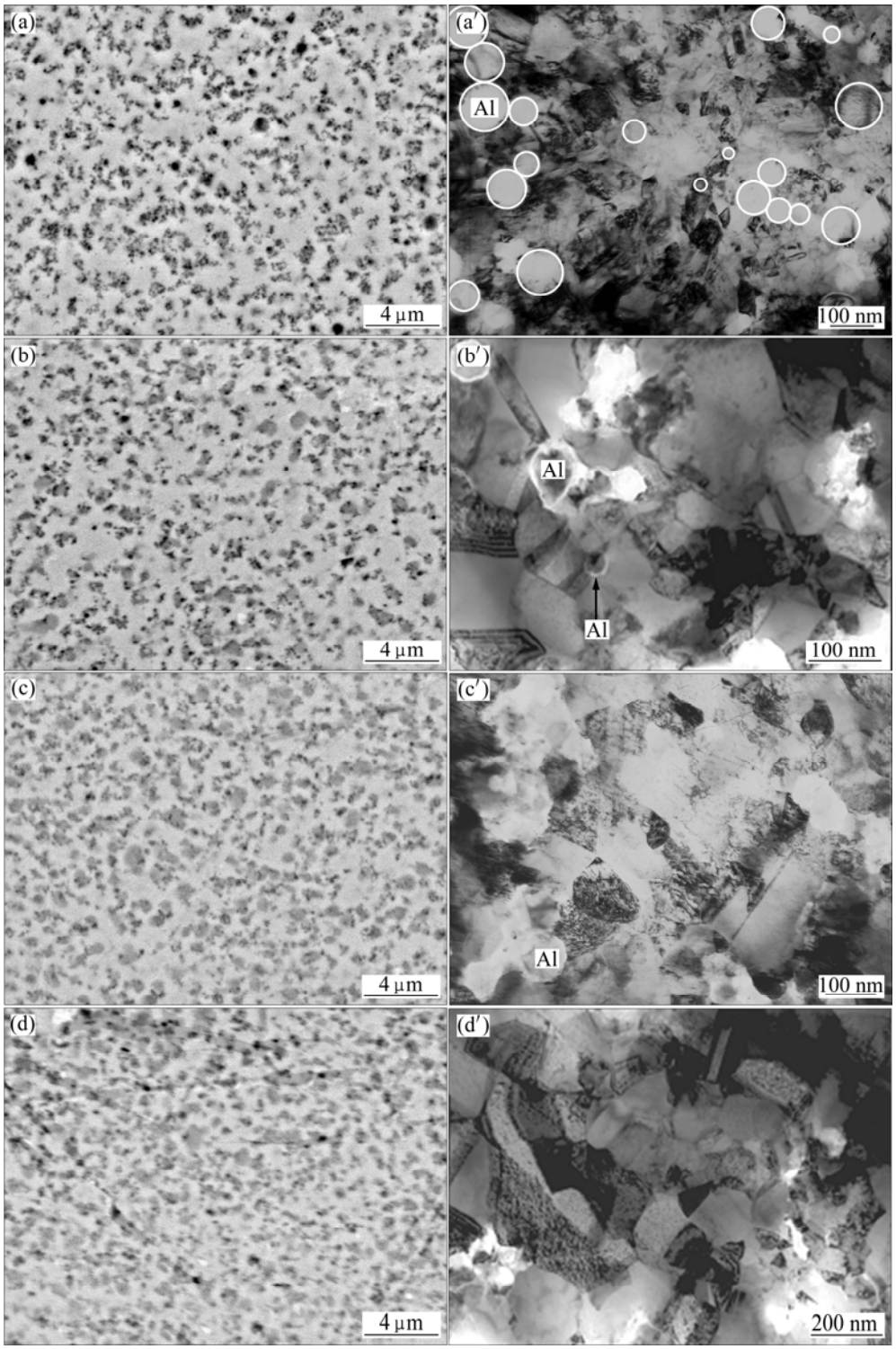

Fig.2 SEM images (polished) (a)−(d) and TEM bright-field images (a′)− (d′) of as-deposited ENC Ni-Al with and without annealing at 500 °C for different time: (a), (a′) 0 h; (b), (b′) 3 h; (c), (c′) 5 h; (d), (d′) 8 h

are visible within the Ni grains. No defects such as pores and cracks are seen in the electrodeposits. The distances between the two neighboring Al nanoparticles, mostly, range from several nanometers to hundreds nanometers. After the annealing treatment, the mean Al content of the three A-ENC Ni-Al coatings was measured using energy-dispersive X-ray analysis (EDAX). The results exhibit that the Al content is about 7.4% (mass fraction, the same below if not mentioned), which is lower than 14.0% Al. The reason is understandable and given in Ref.[19]. Firstly, the as-deposited Ni-Al nanocomposite surface contains certain particles that are loosely attached to the coating, which leads to the fact that the surface Al content is always higher than that in the bulk

nanocomposite. Secondly, the annealing induces consumption of Al in the Ni-Al nanocomposite, due to the inward interdiffusion between the nanocomposite and the underlying nickel, and the outward diffusion to form oxide scales. Thirdly, part nanoparticles in the agglomerated area may not be fully converted into intermetallics phase between Ni and Al. Fig.2(b) shows the SEM morphology of the polished A-ENC after annealing for 3 h. The gray area contains a relatively higher content of Al, indicating that it is δ-Ni_2Al_3 or γ'-Ni_3Al phase in combination with the XRD characterization result. The light area is, γ-Ni matrix with a solid solubility of 5.0%−6.0%Al according to EDAX. Moreover, the annealing causes the coarsening of the nanocrystalline Ni grains of the nanocomposite, from ~40 nm to ~100 nm, based on TEM investigation, as shown in Fig.2(b′). A remarkable increasing of gray area (as shown in Fig.2(c) and Fig.2(d)), the coarsening of the grains and the dispersion of the unsoluble Al nanoparticles (as shown in Fig.2(c′)) were observed with the increase of annealing time. The grains coarsened from 100 nm to ~120 nm and ~200 nm for 5 h and 8 h, respectively, as shown in Fig.2(c′) and Fig.2(d′). However, no unsoluble Al nanoparticles were observed after 8 h annealing, as shown in Fig.2(d′). Voids and micro-cracks extensively occurred at the nickel grain boundaries and at the interfaces between nickel and Al nanoparticles. The result was similar to the previous work[18] but different from the work of YANG et al[19−20]. Investigations[21−23] showed that void formation was related to the condensation of excess vacancies because the phase transformation of Al and Ni to δ-Ni_2Al_3 or γ'-Ni_3Al could cause volume shrinkage. Under the tensile strain, micro-cracks formed.

3.2 Oxidation

Fig.3 shows the mass change vs time curves of various samples in thermal cycling of 40 h in air at 1 000 °C. Clearly, the A-ENC has an oxidation rate much lower than the ENC, the same result as in Ref.[19], due to the accelerated development of the alumina layer on the annealed nanocomposite. In the first 15 h, three A-ENC Ni-Al coatings exhibit similar low mass gains. After 25 h the A-ENC Ni-Al coatings with 5 h annealing treatment continues to oxidize rapidly and spallation of small pieces of scale occurs in the later stage. After 35 h, the mass loss by spallation becomes larger than the mass gain by oxidation. The spallation was also viewed by naked eyes. Only after 15 h, a significant mass gain occurs for the A-ENC Ni-Al with 3 h annealing. The oxidation rate of the A-ENC Ni-Al with 8 h annealing treatment steadily decreases.

The XRD characterization indicates that the oxide phases formed on various samples are composed of Al-rich oxides ($NiAl_2O_4$ and Al_2O_3) and NiO. However, the NiO peaks from the A-ENC Ni-Al with 8 h annealing treatment are weak; while those from the ENC Ni-Al and A-ENC Ni-Al with 3 h and 5 h annealing treatment samples are much stronger, especially the former. This suggests that the annealing treatment significantly suppresses NiO growth during the thermal cycling of the ENC Ni-Al. The latter was also visually confirmed by SEM/EDAX investigation.

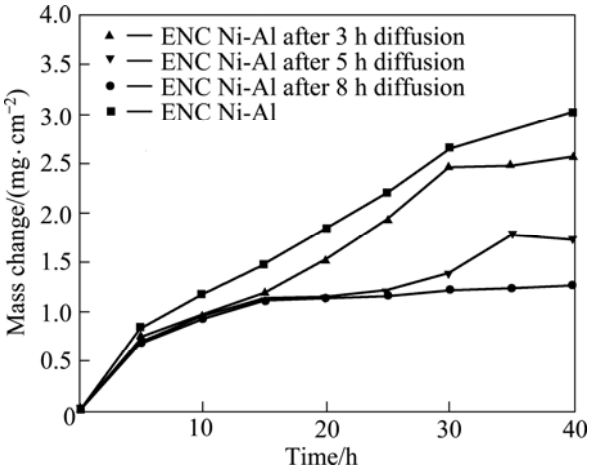

Fig.3 Curves of cyclic oxidation in air at 1 000 °C for as-deposited ENC Ni-Al before and after being annealed at 500 °C for different time

The surfaces morphologies of various samples after cyclic oxidation were investigated by SEM. Heavy spallation and the formation of NiO nodules on spallation area occur on the ENC Ni-Al as presented in Fig.4(a). Fig.4(b) shows a magnified image of the spallation-free area, where large-grained NiO is clearly seen, according to EDAX in combination with XRD characterization. Spallation also occurs on the A-ENC Ni-Al. However, the number and the size of NiO nodules steadily decrease with the increase of the annealing time, as shown in Figs.4(c), (e) and (g). Small NiO grains still form in the spallation-free area for A-ENC Ni-Al with 3 h and 5 h annealing treatment, as shown in Figs.4(d) and (f), respectively. However, Al-rich oxides begin to form in some spallation-free area on the A-ENC Ni-Al with 8 h annealing treatment, as seen in area *B* in Fig.4(h). From the comparison of Figs.4(b), (d), (f) and (h), it is concluded that the annealing treatment decreases the grain size of NiO formed in the spallation-free area and promotes selective oxidation of Al to form a continuous alumina layer[19], which is consistent with the oxidation kinetics in Fig.3.

Fig.5 presents the corresponding cross-sections of the scales passing through NiO nodules. It is found that the number and the size of NiO nodules significantly decrease with the increase of the annealing

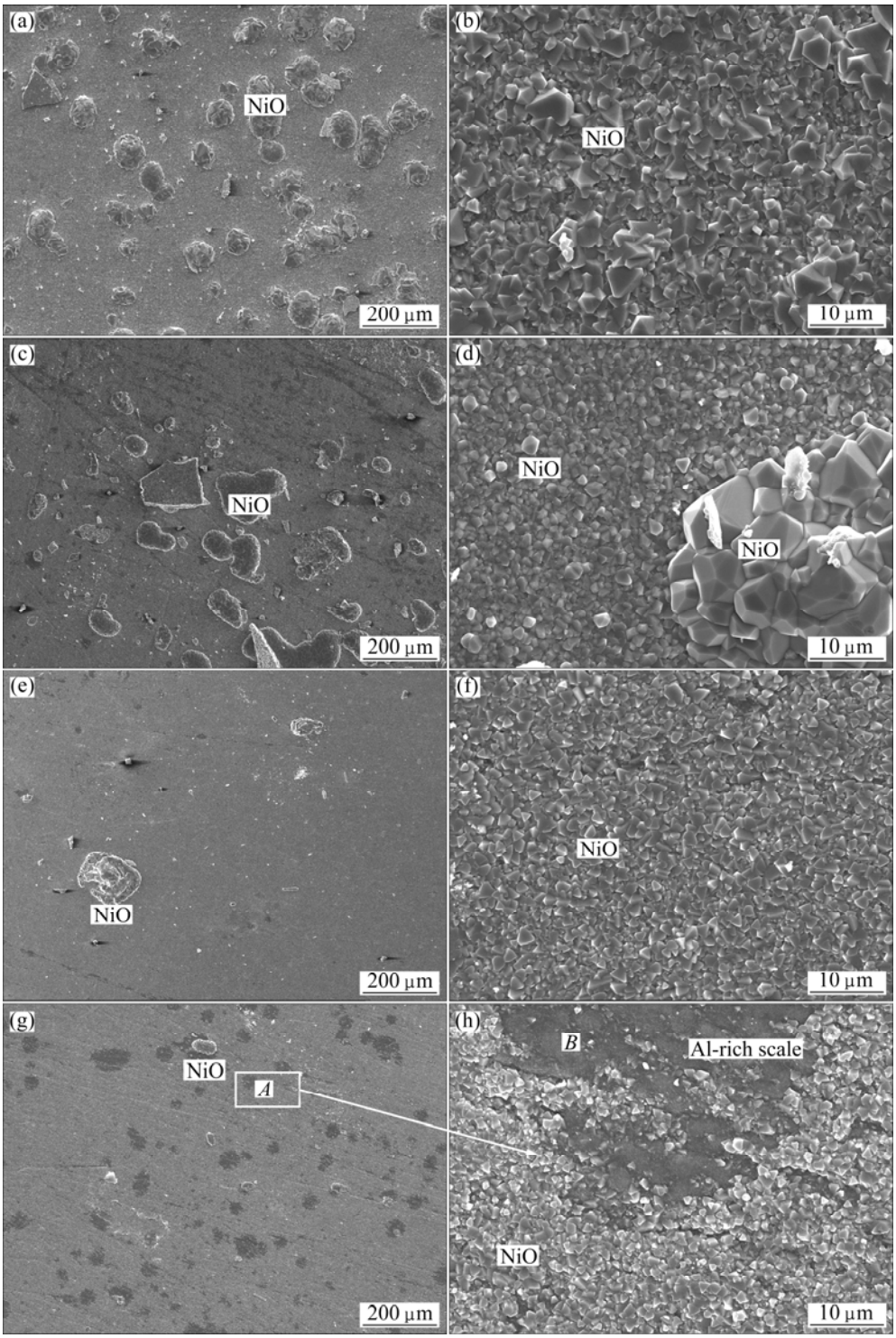

Fig.4 Surface morphologies of oxide scales formed on as-deposited ENC Ni-Al before and after annealing at 500 °C for different time: (a), (b) 0 h; (c), (d) 3 h; (e), (f) 5 h; (g), (h) 8 h

time. From the corresponding high magnified images of the scales formed in the spallation-free area on various samples, it is found that a continuous layer of Al_2O_3 is formed beneath the outer NiO layer. A very thin layer of $NiAl_2O_4$ spinel, which appears darker than outer NiO layer but lighter than inner Al_2O_3 layer in color contrast, is observed between the two layers, based on the investigation of XRD characterization in combination with SEM/ EDAX investigation. Similar structured scale also occurred on the Ni-28%Al nanocomposite after 20 h oxidation[15−16]. Here, it is noteworthy that the top NiO formed is not uniform in thickness and it differs from place to place. However, both the thickness and volumetric fraction of NiO formed

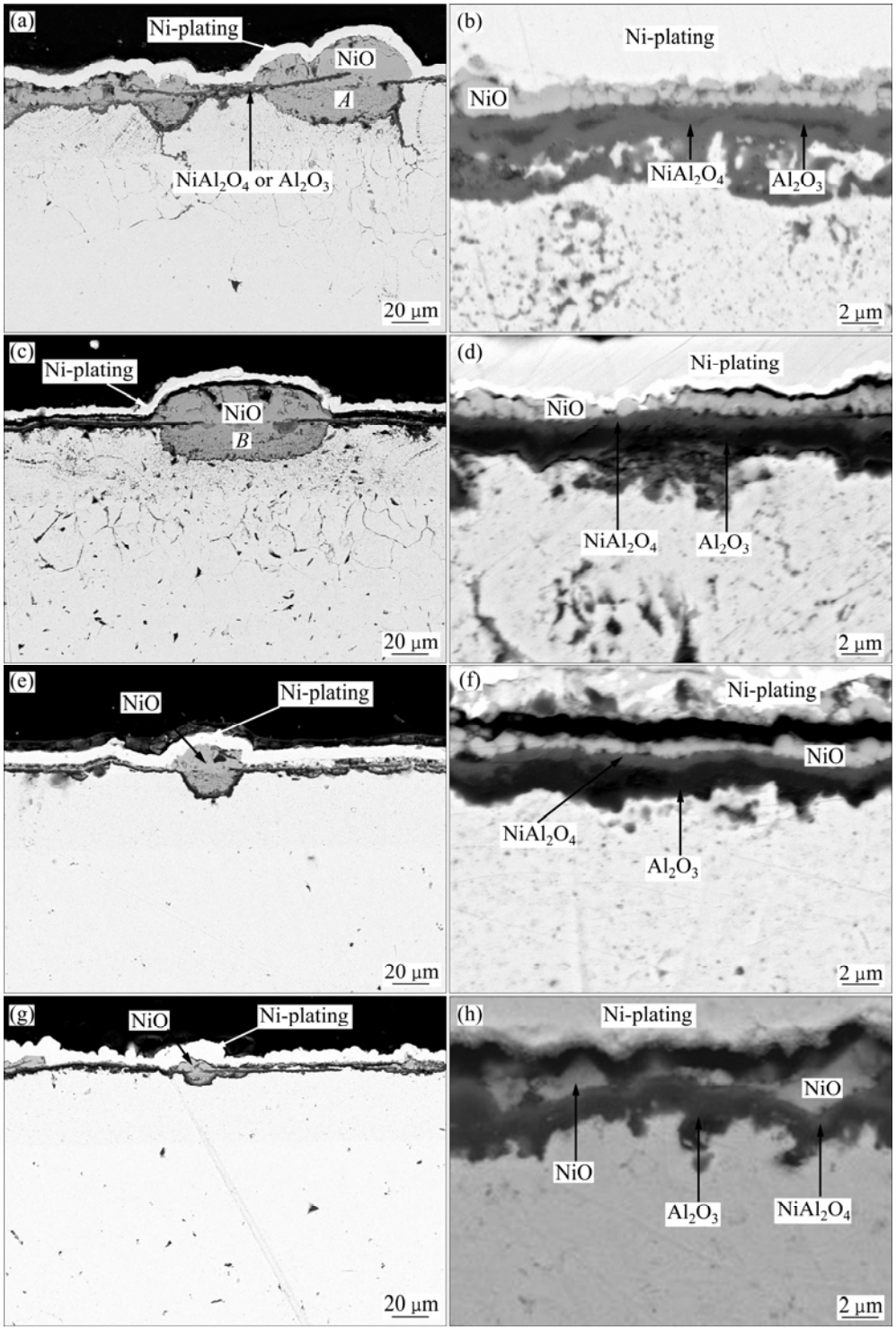

Fig.5 Cross-sectional morphologies of oxide scales formed on as-deposited ENC Ni-Al before and after annealing at 500 °C for different time: (a), (b) 0 h; (c), (d) 3 h; (e), (f) 5 h; (g), (h) 8 h

on the spallation-free area are reduced with the increase of annealing time.

A thin alumina layer can be clearly seen in the middle of the NiO nodule on the ENC Ni-Al and A-ENC Ni-Al with 3 h annealing treatment, as shown in Fig.5(a) and Fig.5(c), respectively. This thin alumina layer is almost parallel to the surface alumina layer around the NiO nodules. At the same time, deep and heavy internal oxidation occurs. The internal oxidation depth far exceeds the nanocomposite thickness of 35 μm. This means that the internal oxidation is extended to the nickel plate substrate. Fig.6 shows a bright-field TEM image of the internal oxidation zone in the Ni plate, where aluminum oxide is formed between the nickel

grains on the basis of the EDAX analysis. The result suggests that the internally-oxidized scales in the nickel plate result from the inward grain boundary diffusion of aluminum from the composite during the cyclic oxidation. Similar NiO nodule and internal oxidation also occur on the Ni-28%Al nanocomposite after 126 h cyclic oxidation at 1 000 °C[18]. From the work, the formation of NiO nodules and internal oxidation relates to the composite intergranular cracking which occurs during the thermal cycling, as addressed below.

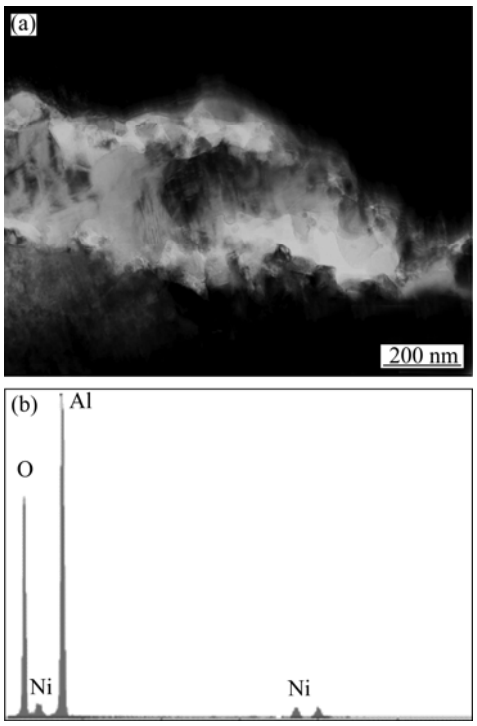

Fig.6 Bright-field TEM image (a) and corresponding EDAX (b) showing formation of internal alumina at grain boundaries of Ni plate

The intergranular crackings of the ENC Ni-Al and A-ENC with 3 h annealing treatment are related to the generation of tensile strain during the thermal cycling. The tensile strain is mainly caused by the volume shrinkage due to the phase transformation from Al nanoparticles and Ni to Ni-Al intermetallics such as δ-Ni_2Al_3 or γ'-Ni_3Al, and the growth of the nanocrystalline nickel grains during oxidation, and by the mismatch in the coefficients of thermal expansion (CTE) between the scale and the nanocomposite during cooling. The TEM image indicates that the grains are coarsened from ~40 nm to the averaged ~100, ~120 and ~200 nm after 3, 5 and 8 h annealing at 500 °C, respectively. Therefore the grain coarsening kinetics is not significant and the strain by the grain growth is ignored. Based on the above analysis, the annealing treatment decreases the tensile strain only from the phase transformation during oxidation for three A-ENC Ni-Al samples. Thus the ENC Ni-Al and A-ENC with 3 h annealing treatment should exhibit extensive tensile strain during cyclic-oxidation due to the lowest alloying. When the tensile strain reaches a critical value, the composite intergranular cracking occurs. The intergranular cracking may extend to the formed scale and the underlying nickel plate. The scale cracking exposes the underlying coating directly to the air during the subsequent cyclic oxidation. Consequently, much thicker NiO outward- or inward-protrusions form on the fresh surface (Fig.4(a) and Fig.4(c)) because the aluminum content beneath the scale is too low and it cannot be compensated by the fast supply of aluminum from the coating due to the coarsening of the nanocrystalline grains. The inward-protruded NiO, different from the oxide formed on the other area, is incorporated by minor Al-rich oxides ($NiAl_2O_4$ and/or Al_2O_3), as shown in area *A* in Fig.5(a). Simultaneously, once the through-scale cracks occur, gas oxygen inward penetrates through the cracks produced in the composite and the underlying Ni plate, causing internal oxidation of aluminum.

For the A-ENC coatings with 5 h and 8 h annealing, the tensile strain source is the mismatch in the coefficients of thermal expansion (CTE) between the scale and the nanocomposite during oxidation, and the oxides scale cracking in cooling, which leads to the formation of the NiO nodules. When oxidation continues, the advancement of the NiO inward-protrusions progressively decreases the partial pressure of oxygen and simultaneously increases the Al content at the oxidation front, which leads the selective oxidation of Al to form a continuous alumina layer (Figs.5(e) and (g)). Afterward, the NiO growth is completely prevented, leading to the improvement of the oxidation resistance.

4 Conclusions

1) The electrodeposited nanocomposite of Ni-14%Al is composed of nanocrystalline Ni matrix and dispersed Al nanoparticles. After the annealing treatment in vacuum at 500 °C, the nanocomposite can be transformed into δ-Ni_2Al_3 + γ'-Ni_3Al+γ-Ni composite, in which the Ni grains are coarsened but still ultrafine size, and simultaneously they are incorporated by an appropriate amount of solute Al atoms.

2) The volume fraction of γ'-Ni_3Al increases with the increase of the annealing time.

3) Cyclic oxidation at 1 000 °C shows that the scale spallation resistance of the A-ENC Ni-Al increases with the increase of annealing time, due to the prevention of the formation of numerous surface NiO nodules and internal oxidation of aluminum as a result of the composite intergranular cracking during the cycling.

References

[1] WU G, LI N, ZHOU D R, MITSUO K. Electrodeposited Co-Ni-Al_2O_3 composite coatings [J]. Surface and Coatings Technology, 2004, 176: 157−164.

[2] ZHANG Wen-feng, ZHU Di. Oxidation behavior of Ni-ZrO_2 nano-composite electroforming deposits at high temperature [J]. Transaction of Materials and Heat Treatment, 2006, 27(5): 114−117. (in Chinese)

[3] ZHOU Yue-bo, ZHANG Hai-jun. Oxidation resistance of electrodeposited Ni-Al_2O_3 nanocomposite coating [J]. Transaction of Materials and Heat Treatment, 2008, 29(2): 154−157. (in Chinese)

[4] PENG Xiao, LI Tie-fan, LI Mei-shuan, MA Xin-ging, PING De-hai. Effect of Ni-La_2O_3 electrodeposited composite film on thermal cycling oxidation of Ni [J]. Acta Metallurgica Sinica, 1996, 32(2): 180−186. (in Chinese)

[5] ZHOU Yue-bo, DING Yuan-zhu. Oxidation resistance of the co-deposited Ni-SiC nanocomposite coating [J]. Transactions of Nonferrous Metals Society of China, 2007, 17(5): 925−928.

[6] BI Xiao-qin. Effects of technology parameters on microstructures and properties of Ni-Sic composite coatings [J]. Journal of Materials Engineering, 2007(5): 39−42. (in Chinese)

[7] STOTT F H, ASHBY D J. The oxidation characteristics of electrodeposited nickel composites coating containing silicon carbide particles at high temperature [J]. Corrosion Science, 1978, 18: 183−198.

[8] FOSTER J, CAMERON B P, CAREW J A. The production of multi-component alloys coatings by particle codeposition [J]. Trans Inst Met Finish, 1985, 63: 115−119.

[9] IZAKI M, FUKUSUMI M, ENOMOT H. High temperature oxidation resistance of Ni-Al alloy films prepared by heating electrodeposited composite [J]. J Japan Inst Met, 1993, 57: 182−189.

[10] SUSAN D F, MARDER A R. Oxidation of Ni-Al-based electrodeposited composite coatings Ⅰ: Oxidation kinetics and morphology at 800 °C [J]. Oxid Met, 2002, 57: 131−157.

[11] SUSAN D F, MARDER A R. Oxidation of Ni-Al-based electrodeposited composite coatings Ⅱ: Oxidation kinetics and morphology at 1 000 °C [J]. Oxid Met, 2002, 57: 159−180.

[12] LIU H F, CHEN W X. Cyclic oxidation behavior of electrodeposited Ni_3Al-CeO_2 base coatings at 850 °C [J]. Oxid Met, 2005, 64: 331−354.

[13] LIU H F, CHEN W X. Cyclic oxidation behaviour of electrodeposited Ni_3Al-CeO_2 base coatings at 1 050 °C [J]. Corrosion Science, 2007, 49: 3453−3478.

[14] ZHOU Y B, ZHAO G G, ZHANG H J. Effect of CeO_2 on the microstructure and isothermal oxidation of Ni-Al alloy coatings transformed from electrodeposited Ni-Al films at 800 °C [J]. Vacuum, 2009, 83: 1333−1339.

[15] ZHOU Y, PENG X, WANG F. Size effect of Al particles on the oxidation of electrodeposited Ni-Al composite coatings [J]. Oxid Met, 2005, 64: 169−183.

[16] ZHOU Y, PENG X, WANG F. Oxidation of a novel electrodeposited Ni-Al nanocomposite film at 1 050 °C [J]. Scripta Materialia, 2004, 50: 1429−1433.

[17] ZHOU Y B, QIAN B Y, ZHANG H J. Al particles size effect on the microstructure of the co-deposited Ni-Al composite coatings [J]. Thin Solid Films, 2009, 517: 3287−3291.

[18] ZHOU Y, PENG X, WANG F. Cyclic oxidation of alumina-forming Ni-Al nanocomposites with and without CeO_2 addition [J]. Scripta Materialia, 2006, 55: 1039−1042.

[19] YANG X, PENG X, WANG F. Effect of annealing treatment on the oxidation of an electrodeposited alumina-forming Ni-Al nanocomposite [J]. Corrosion Science, 2009, 50: 3227−32.

[20] YANG X, PENG X, WANG F. Size effect of Al particles on the structure and oxidation of Ni/Ni_3Al composites transformed from electrodeposited Ni-Al films [J]. Scripta Materialia, 2007, 56: 509−512.

[21] LIU H F, CHEN W X. Reactive oxide-dispersed Ni_3Al intermetallic coatings by sediment co-deposition [J]. Intermetallics, 2005; 13: 805−817.

[22] SUSAN D F, MISIOLEK W Z, MARDER A R. Reaction synthesis of Ni-Al-based particle composite coatings [J]. Metall Mater Trans A, 2001, 32: 379−390.

[23] SUSAN D F, MARDER A R. Ni-Al composite coatings: Diffusion analysis and coating lifetime estimation [J]. Acta Materialia, 2001, 49: 1153−1163.

退火处理对 Ni-Al 纳米复合镀层循环氧化性能的影响

周月波，张海军

黑龙江科技学院 材料科学与工程学院，哈尔滨 150027

摘　要：研究在 500 °C 真空扩散不同时间条件下的扩散合金化对 Ni-Al 纳米复合镀层的结构与抗循环氧化性能的影响。结果表明：扩散不仅导致 Ni-Al 纳米复合镀层的基体 Ni 晶粒粗化，还导致 Al 固溶在基体 Ni 中，Ni 与 Al 之间形成金属化合物；随着扩散合金化时间的延长，Ni-Al 合金涂层中的空洞减少，从而减少了合金涂层在循环氧化过程中出现的穿透性裂纹和内氧化，抑制了氧化膜剥落区瘤状 NiO 的形成，提高了 Ni-Al 合金涂层的抗循环氧化性能。

关键词：电镀；纳米涂层；循环氧化

(Edited by LI Xiang-qun)